The 2023 World Congress on
Advances in Structural Engineering and Mechanics (ASEM23)
GECE, Seoul, Korea, August 16-18, 2023

Investigation of Size Effect Phenomenon in Split Tension Testing: An Experimental and Numerical Study

* Hemam Amarjit Singh[1)], Rukhsar Ahmed[2)], Rimen Jamatia[3)]

[1), 2), 3)]*Department of Civil Engineering, Indian Institute of Technology Jammu, Jammu and Kashmir, India, 181221.*
[1)]*hemam.singh@iitjammu.ac.in,* [2)] *2020PCE1007@iitjammu.ac.in,*
[3)] *rimen.jamatia@iitjammu.ac.in*

ABSTRACT

This study presents a comprehensive investigation of the size effect phenomenon in cylindrical specimens using the split tensile test. Experimental analysis was performed on cylindrical samples of different diameters (150 mm, 300 mm, and 500 mm), considering a maximum aggregate size of 10 mm. 2D plane strain numerical simulations using the Finite element method (FEM) were conducted to explore the size effect phenomenon further, extending the specimen diameters to 700 mm, 1000 mm, 1200 mm, and 1500 mm. The simulations incorporated the concrete damage plasticity (CDP) model as the material constitutive model. The results indicate a minimal decrease in tensile strength with increasing size, suggesting a limited size effect on nominal strength. Furthermore, the study explored the effects of crack geometry by introducing notches at different positions and orientations in the numerical simulations. The study also investigated the effect of varying fracture energy on the size effect phenomenon. Notch placement at a 45-degree angle at the end of the loading tips notably reduces tensile strength with increasing size while decreasing the fracture energy intensifies this effect. These findings highlight the significance of notch characteristics and fracture energy in understanding the size effect phenomenon.

1. INTRODUCTION

A significant factor influencing the behavior of concrete and other quasi-brittle materials is the size effect phenomenon, which refers to variations in mechanical behavior with changes in structural sizes. Concrete, being a widely used construction material, exhibits complex mechanical responses due to its composition of cement paste, aggregates, water, micro-cracks, and other constituents (Häfner et al., (2006); Du et al., (2013)). Various experimental and simulation studies have been conducted to investigate the size effect of concrete materials (Bazant et al. (1991); Lessard et al. (1993); Zhou et al. (1998); Kim et al. (2000); Ince and Arici (2004); Carmona (2009); Sim et al. (2013);

Jin et al. (2020)).

To study the size effect of tensile strength on concrete specimens, splitting tensile tests were employed in place of direct tensile tests (Malhotra (1976); Rocco et al. (1999); Wang et al. (2014); Murali and Deb (2017)). These tests have revealed how concrete materials behave regarding tensile strength and size effects. For instance, Malhotra (1976) conducted splitting tensile tests on two different sizes of cylindrical specimens and discovered that smaller specimens exhibited higher nominal strengths compared to larger specimens. On the other hand, Rocco et al. (1999) found that the tensile strength of concrete decreased as the specimen size increased. These results were supported by Wang et al. (2014), Murali and Deb (2017); and Zhang et al. (2016). However, the topic still holds some discrepancies and arguments due to variations in experimental results. Zhou et al. (1998), Hasegawa et al. (1985), Bažant et al. (1991) reported a conflict finding, observing a reversal in the size effect. These differences highlight the importance of conducting a thorough analysis to fully comprehend the effects of concrete size on splitting tensile strength.

Numerical simulations have become an important tool for understanding the size effect phenomenon. The Finite Element Method (FEM) simulations have enabled researchers to study the size effect on concrete specimens beyond experimental limitations, allowing exploration of a wider range of geometries. Numerical simulations by Murali and Deb (2017) showed a size effect reversal for certain meso geometries in split cylinder specimens. Jin et al. (2020) found that splitting tensile strength decreased as the cube side length increased, especially for smaller maximum aggregate sizes (MAS). Carmona (2009) focused on the notch effect, emphasizing the importance of considering geometric irregularities. However, as indicated by Simone et al. (2004), Jirásek et al. (2004)), Kravani et al. (2009), certain models exhibited discrepancies in accurately capturing the size effect. This emphasizes the importance of further research to address these discrepancies and enhance the model's capability to consistently predict size-dependent behavior in concrete structures.

The objective of this study is to make a significant contribution to the investigation of the size effect phenomenon in concrete materials. The research involves both experimental analysis and numerical simulations, specifically focusing on the tensile strength size effect in cylindrical concrete specimens. The experimental study includes testing cylindrical samples ranging from 150 mm to 500 mm in diameter using split tensile tests. Subsequently, 2D plane strain numerical simulations are conducted with Finite Element Method (FEM) to extend the specimen diameters up to 1500 mm, utilizing concrete damage plasticity as the material constitutive model. The research also delves into the effect of notches on the size effect phenomenon in concrete materials, aiming to understand how geometric irregularities influence the size effect response. Additionally, the study investigates the effect of fracture energy in the size effect analysis. By combining experimental and numerical approaches, this research seeks to gain comprehensive insights into the size effect phenomenon in split tensile testing for concrete materials.

2. Experimental Analysis

To investigate the size effect in the split tensile test of concrete, cylindrical concrete specimens were prepared with maximum aggregate sizes of 10 mm. Three sets of specimens with diameters of 150 mm, 300 mm, and 500 mm, and a constant height of 100 mm, were considered, with each set consisting of three different sizes. In total, 18 specimens were cast. The specimens were made using a nominal mix of M20 concrete, maintaining a water-cement ratio of 0.6, and a cement to fine aggregate to coarse aggregate ratio of 1:1.5:3. To assess the concrete's strength, compression tests were conducted on standard cylindrical samples with a diameter of 150 mm and a height of 300 mm, consisting of six cylinders. After 28 days of curing, the average compressive strength of the concrete was measured as 23.26 MPa.

2.1 Testing Setup

The compressive testing machine with a load capacity of 500kN was utilized to perform the tests. A steel plate of width (2b) and a height of 100 mm, maintaining a width/diameter ratio of 0.1, conforming to IS 5816:1999, was positioned between the pressure plates and the cylindrical specimen, as shown in Fig. 1. The specimen intended for splitting tensile tests underwent continuous and uniform loading without experiencing any impact. The loading rate was regulated by applying a displacement of 0.5 mm/min. The load was incrementally increased until the specimen failed diametrically. The failure load was then recorded. The displacement was measured using Linear Variable Differential Transformers (LVDTs).

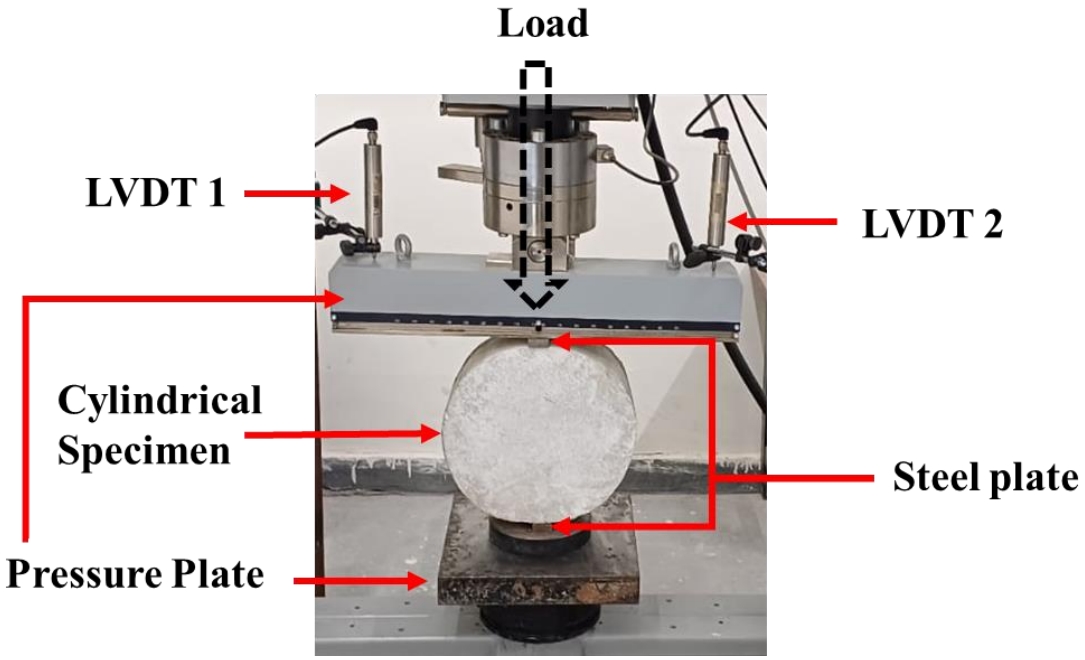

Fig. 1 Experimental setup of concrete for splitting tensile test.

2.1 Tensile Strength

The average splitting tensile strength was determined by converting the ultimate load at failure to the nominal tensile strength using the formula, $\sigma_t = 2P/\pi Dt$, where P represents the ultimate load (N), t is the specimen thickness (mm), and D is the specimen diameter (mm). Therefore, D150, D300, and D500 refer to cylindrical specimens with diameters of 150 mm, 300 mm, and 500 mm, respectively. Table 1 presents the average parameters that describe the splitting tensile performance. Notably, all the coefficients of variation for the splitting tensile strengths were below 11%. This indicates that the experimental data in this study exhibited minimal variability, and the obtained test results are considered acceptable.

The experimental study revealed a minimal difference in tensile strength among the tested specimens. However, due to inherent constraints in the experimental setup, it was not feasible to investigate the size effect phenomenon beyond cylindrical concrete specimens with a diameter of 500 mm. Numerical simulations were employed to overcome this limitation and delve deeper into the size effect phenomenon. Through the Finite Element Method (FEM) simulations, the specimen size was extended up to 1500 mm in diameter. This allows to investigate thoroughly the size effect phenomenon under split tension loading.

Table 1: The average tensile strength (σ_t), standard deviation (S), and coefficient of variation (C_v) of the split tensile test.

Name	σ_t (MPa)	S (MPa)	C_v (%)
D150	2.56	0.267	10.42
D300	2.52	0.258	10.25
D500	2.45	0.256	10.45

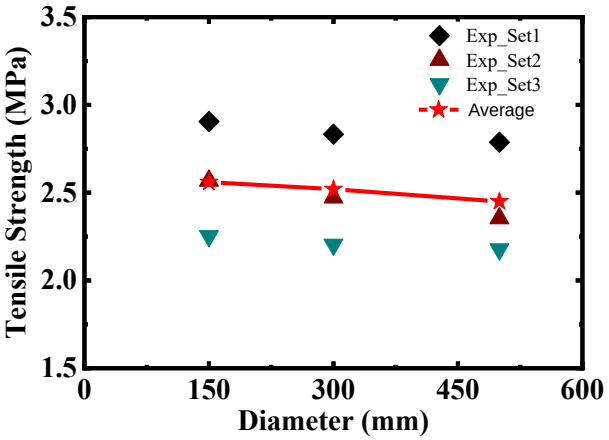

Fig. 2 Variation of tensile strength with diameter

2. Numerical Simulation

This study performs numerical simulations of a split tensile test using ABAQUS, a finite element method (FEM) based software, with a plain strain configuration. The simulation employs the 2D four-node quadrilateral reduced-integration element CPE4R with a mesh size of 3 mm, determined based on the strip width of the smallest specimen (7.5 mm). To ensure mesh convergence, the simulation is validated, as depicted in Fig. 7. The concrete model considered in the simulation is a flattened model, where the length of the flatten is equal to the width of the strip (2b), as depicted in Fig. 3. This flattened concrete model is preferred due to the minimal deformation experienced by the rigid steel strips used as platens, which possess a higher modulus of elasticity compared to concrete. Consequently, the flattened model accurately represents the behavior observed in the numerical simulations as the cylindrical concrete specimen undergoes deformation and conforms to the shape of the flat steel platen during loading. The bottom flat portion of the specimen is constrained in both lateral and axial direction. Uniaxial displacement load is applied in the top flat portion of the specimen to induce the desired tensile stress, as shown in Fig. 3.

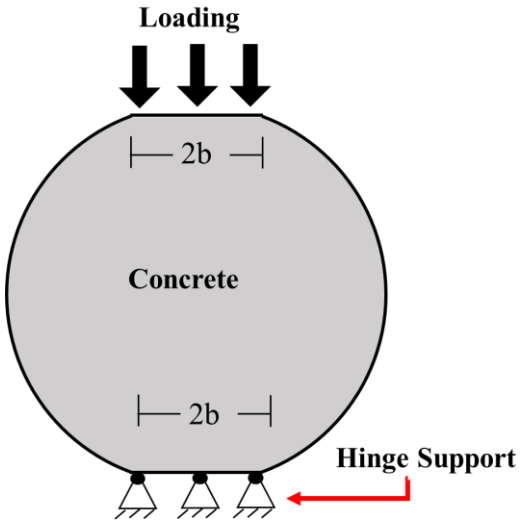

Fig. 3 Macroscale model of flatten concrete under split tension load

3.1 Constitutive model and material property

The constitutive material model plays a pivotal role in the simulation. It accurately represents material behavior, including stress-strain response, crack initiation, and propagation. The concrete damage plasticity (CDP) model is widely used to characterize the mechanical behavior of concrete-like materials, and it is readily available in the ABAQUS material library. In this study, CDP constitutive model is adopted to describe the concrete's damage behavior. This model is a non-associative plasticity model that incorporates the hyperbolic Drucker-Prager flow criterion and the modified Drucker Prager yield criterion. It accounts for the different mechanical behaviors of concrete under

tension and compression, with tension being governed by fracture damage and compression dominated by plasticity. Consequently, the model assesses damaged states separately for tension and compression by using two distinct equivalent plastic strains. These equivalent plastic strains dictate how the yield surface evolves during plastic flow and how the elastic material's strength degrades due to the accumulation of tensile damage caused by crack growth. The yield function (F) can be represented in terms of effective stresses as follows:

$$F = \frac{1}{1-\alpha}\{\bar{q} - 3\alpha\bar{p} + \beta(\bar{\epsilon}^{pl})\langle\bar{\sigma}_{max}\rangle - \gamma\langle\bar{\sigma}_{max}\rangle\} - \bar{\sigma}_c(\bar{\epsilon}^{p}) \quad (1)$$

Where, $\bar{q} = \sqrt{\frac{3}{2}\bar{S}:\bar{S}}$ is the mises equivalent effect stress, $\bar{S}$ is the effective deviator stress and $\bar{p}$ is the hydrostatic pressure. In-depth details information on the CDP can be found in the ABAQUS documentation.

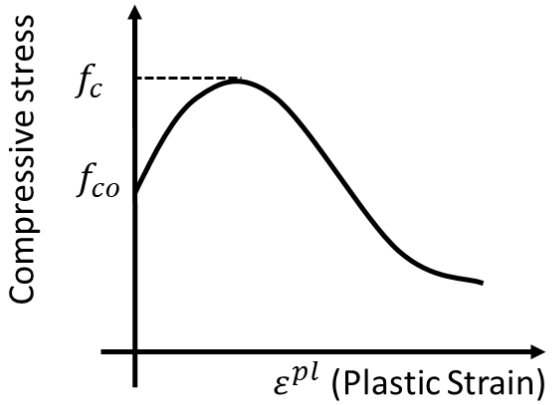

Fig. 4 Inelastic stress-strain curve under compression

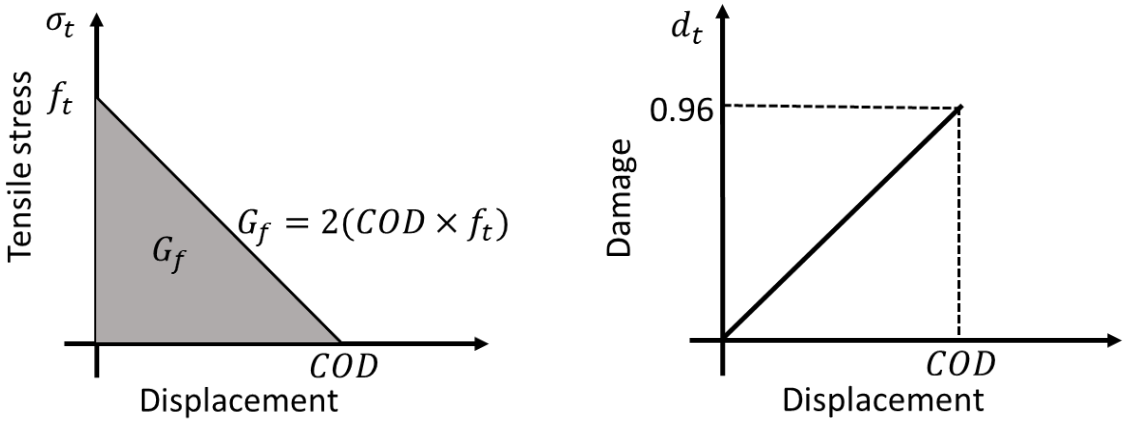

Fig. 5 Cracking displacement-stress curve (left) and displacement-damage (right) under tension.

In this study, the inelastic stress-strain compression is generated by using the stress-strain relation develop by Saenz (1964) (Eq. (2)).

$$\sigma_c = \frac{E_o \varepsilon_c}{1+\left(\frac{E_o \varepsilon_p}{\sigma_p}-2\right)\left(\frac{\varepsilon_c}{\varepsilon_p}\right)+\left(\frac{\varepsilon_c}{\varepsilon_p}\right)^2} \quad (2)$$

Where σ_c and ε_c represent the compressive stress and strain respectively, while σ_p and ε_p are the maximum stress and its corresponding strain. The value for σ_p and ε_p are taken as cylinder compressive strength, f_c and 0.002, respectively. The elastic modulus, $E_o$of the concrete is estimated using the equation, $E_o = 4730\sqrt{f_c}$. Van Mier (1996) argues that tensile crack growth is responsible for compressive failure rather than compression crushing. So, concrete crushing damage parameters due to compression has been ignored. Linear tensile stress and crack opening displacement (COD) curve was used to define the tension stiffening of the concrete. COD can be figured out by knowing the area enclosed by tensile stress and COD, known as fracture energy (G_f) (Fig. 5). According to CEB-FIP, $G_f = 73.0(f_c)^{0.18}$ N/m. The compressive strength (f_c) and tensile strength (f_t) has been considered based on the experiment results obtained from the standard compressive and split tensile tests (Table 2). The tensile damage is calculated as, $d_t = 1 - \sigma_t/f_t$.

Table 2: Material Properties of the macroscale model

Parameters	Value
Compressive strength, MPa	24.00
Tensile strength, MPa	3.5
Fracture Energy, N/m	129.35
Poisson's Ratio	0.2
Elasticity, GPa	23.17

3.1 Concrete material calibration

The model is calibrated by comparing the axisymmetric response with the experimental stress-strain curves obtained from standard cylindrical samples tested under uniaxial compression load. The numerical simulation correlates satisfactorily with the experimental responses (Fig. 8). Additionally, the model is further calibrated using tensile strength data from various specimen sizes, and the numerical simulations exhibit good agreement with the corresponding experimental analyses (Fig. 10).

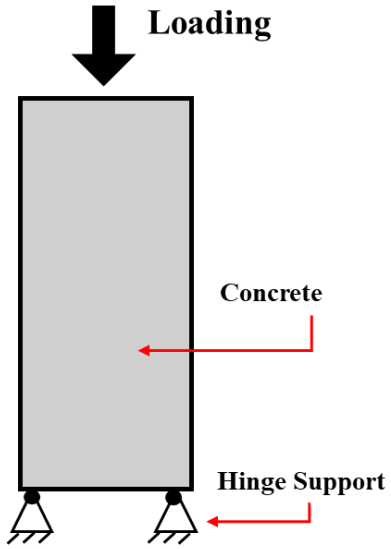

Fig. 6 Axisymmetric model of macroscale concrete under compressive load

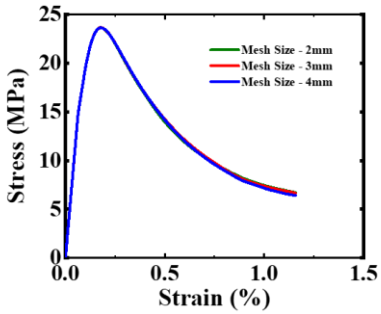

Fig. 7 Compressive stress-strain response of different mesh size.

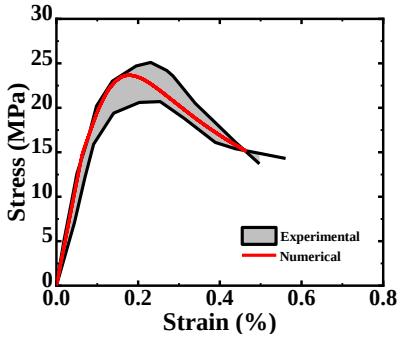

Fig. 8 Numerical calibration of compressive response with experimental data.

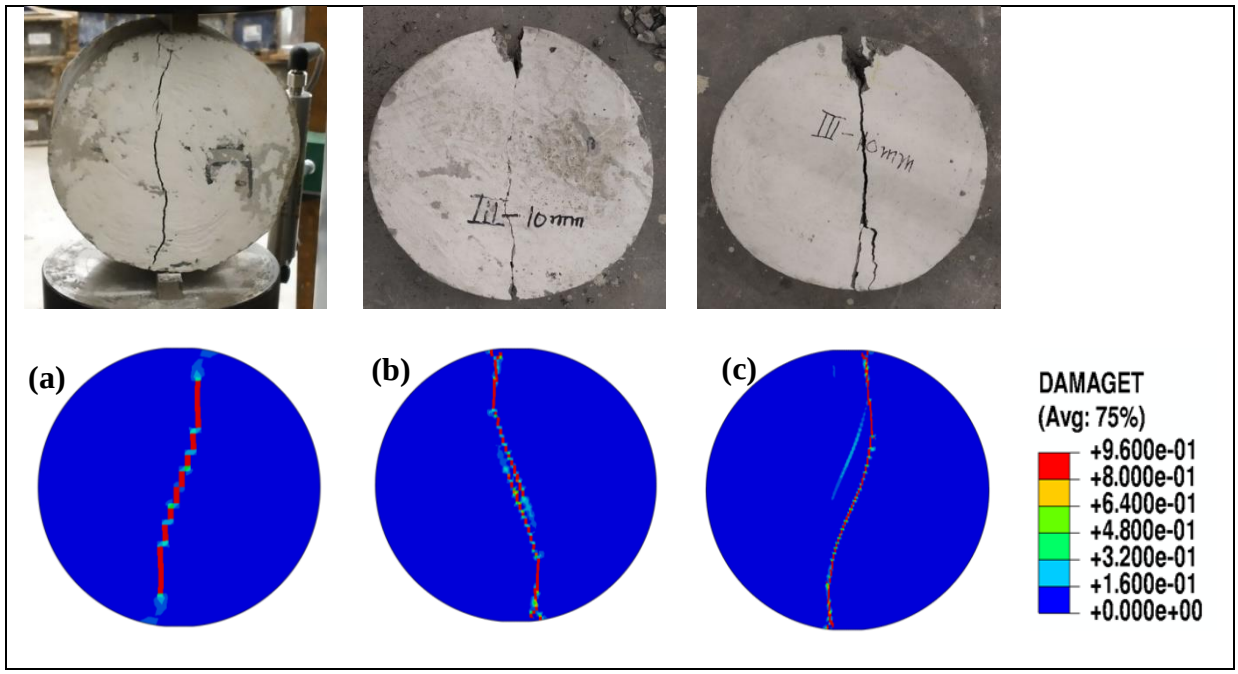

Fig. 9 Failure Pattern in experimental (top) and numerical analysis (bottom) for (a) 150 mm (b) 300 mm and (c) 500 mm diameters under split tension test.

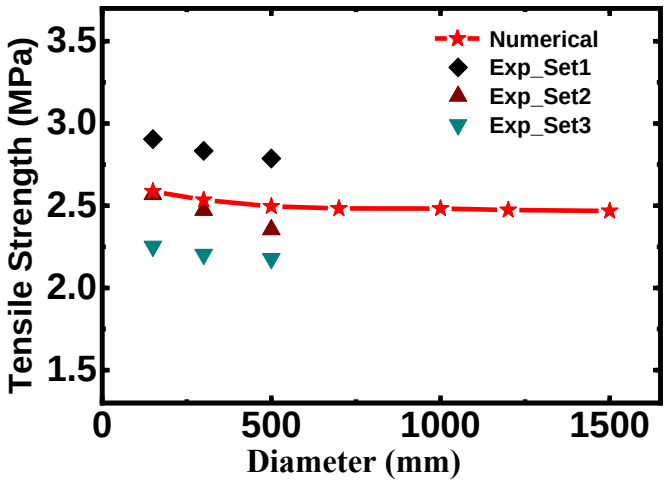

Fig. 10 Comparing Numerical and Experimental Tensile Strength by Diameter.

3.2 Results and Discussion

Flattened circular concrete specimens with various diameters (D = 150 300, 500, 700, 1000, 1200, and 1500 mm) were utilized to investigate the size effect phenomenon on the split tensile test of concrete. To ensure a consistent stress state, self-similar flattened strips were employed. In Fig. 10, a distinct trend emerges as the tensile strength gradually declines until reaching a diameter of 700 mm, after which it stabilizes at a constant value. The observed variations in strength are primarily governed by the mechanisms of damage dissipation and plastic dissipation. A more detailed explanation of these phenomena is provided in the subsequent section.

3.2.1 Damage Dissipation Energy

The top flattened surface of the concrete specimen experiences a uniformly distributed load, leading to the development of a stress field within the specimen. When the axial stress exceeds the material's tensile strength, damage will initiate and propagate due to the available fracture energy. Fig. 11, demonstrates that damage initiation starts at the boundary of the flattened strip. As the load continues to be applied, the maximum damage tends to occur at the center of the specimen, eventually connecting with the boundary crack and dividing the specimen into two halves.

The stress condition at the specimen's boundary is primarily dominated by compressive stresses, both longitudinally and laterally. However, at the center of the specimen, the longitudinal stresses are compressive, while the lateral stresses become tensile (Bazant et al. (1991)). This configuration contributes to the observation of maximum damage at the center of the specimen. As the specimen sizes increase, the strain energy and the dissipation of damage energy also increase (Fig. 12). Consequently, a decrease in tensile strength relative to the specimen size is observed.

3.2.2 Plastic Dissipation Energy

The plastic dissipation energy represents the energy absorbed by the material during plastic deformation, and it is observed to be higher in larger specimen sizes than smaller ones, as depicted in Fig. 12. In larger specimens, the stress and strain fields are distributed over a larger area, causing a more gradual and dispersed strain localization pattern, which enhances the effective dissipation of plastic energy throughout the specimen.

As the size of the specimen increases, there is a corresponding increase in the accumulated strain energy within the element. Additionally, the damage dissipation energy and plastic dissipation energy increase with specimen size. However, it is essential to note that the contribution of damage dissipation to overall energy dissipation becomes relatively less significant than plastic dissipation as the specimen sizes increase. This phenomenon explains the observation of a constant strength after reaching a specimen diameter of 700 mm.

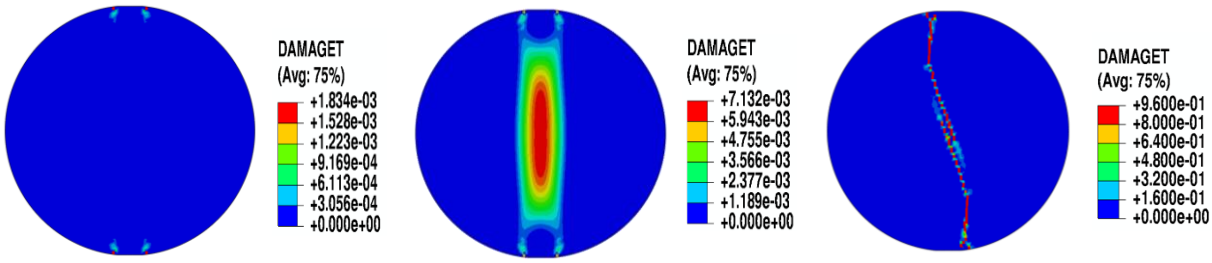

Fig.11 The crack initiation and propagation contour of concrete with a 300 mm diameter under split tension load.

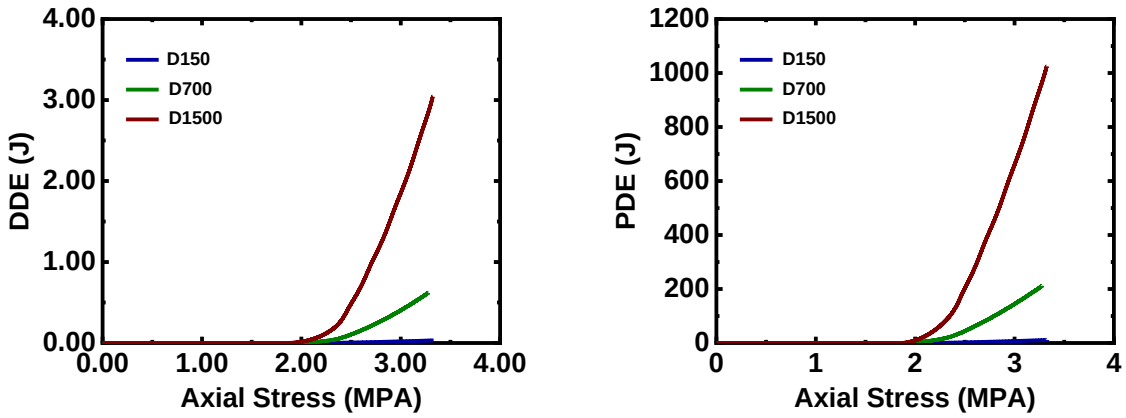

Fig. 12 (a) Damage Dissipation Energy (DDE) and (b) Plastic Dissipation Energy (PDE) of concrete under split tension load.

4. Effect of Pre-existing crack in the size effect study

To thoroughly study how pre-existing cracks affect the size effect, the research includes three different types of self-similar notches. These notches include a centrally located notch parallel to the loading direction (referred to as NC), a 45-degree inclined notch at the center (referred to as INM), and a 45-degree inclined notch positioned at the end of the loading tips (referred to as INT), as depicted in Fig. 13.

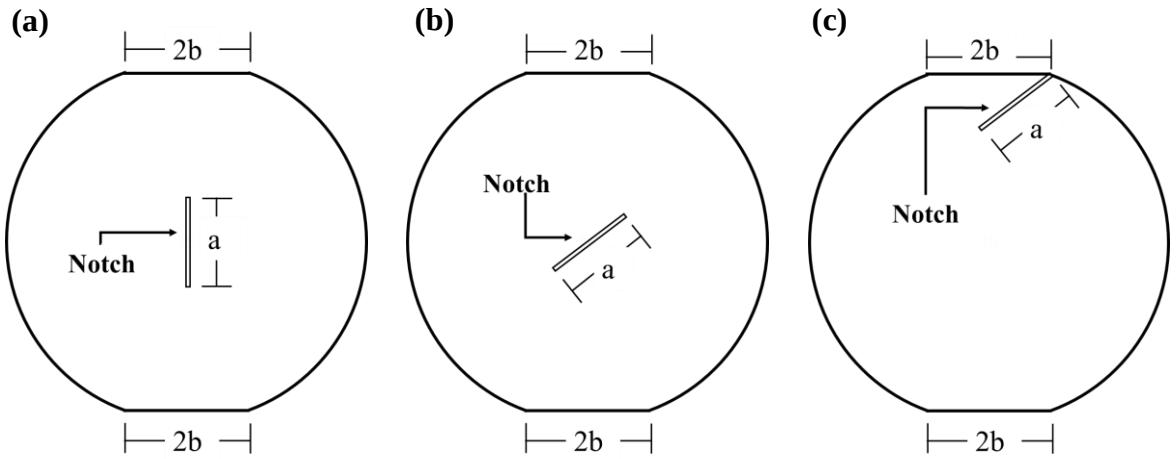

Fig. 13 A visual representation of (a) Centrally situated notch oriented parallel to the loading direction, (b) inclined notch place at the center, and (b) inclined notch place at the end of the loading tips

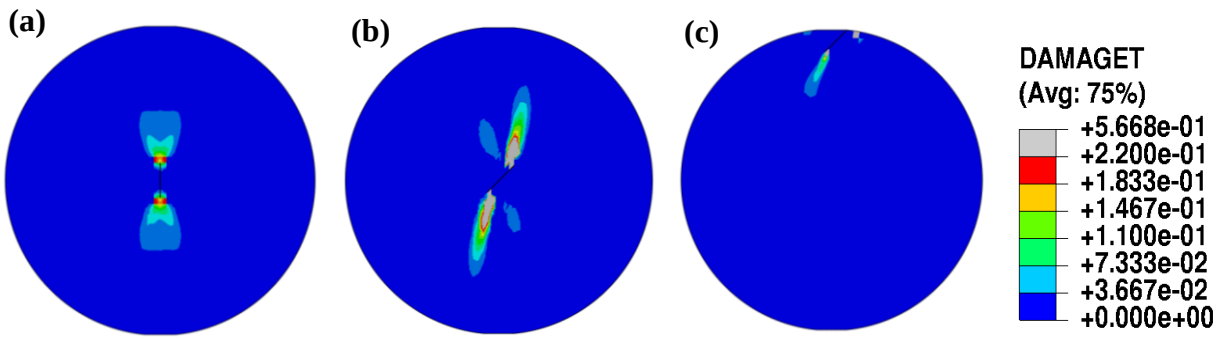

Fig. 14 Damage initiation of (a) Centrally situated notch oriented parallel to the loading direction, (b) inclined notch place at the center, and (b) inclined notch place at the end of the loading tips under split tensile test.

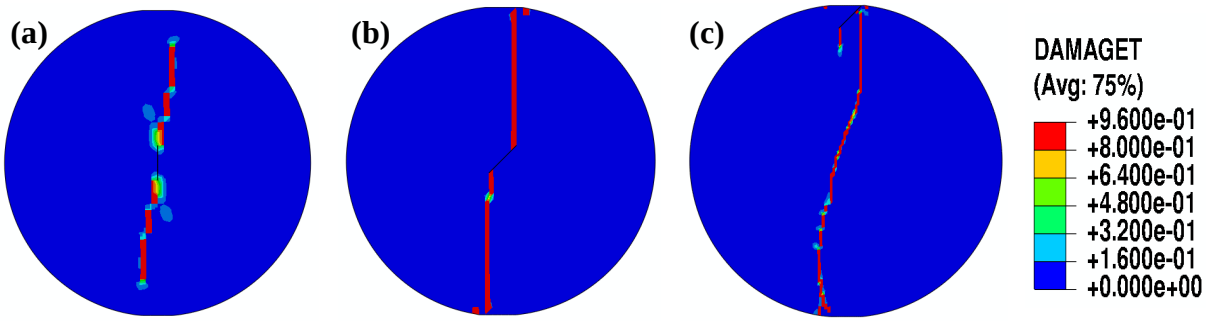

Fig. 15 Damage propagation of (a) Centrally situated notch oriented parallel to the loading direction, (b) inclined notch place at the center, and (b) inclined notch place at the end of the loading tips under split tensile test.

The presence of a notch disrupts the continuity of the material. It creates a highly localized stress concentration at the notch tips, resulting in a higher likelihood of crack initiation and propagation from the notch tips (Fig. 14). However, the presence of inclined notches significantly influences the tensile strength of the material. In addition to the normal stresses, inclined notches introduce shear stresses, creating a complex stress state within the material. These combined normal and shear stresses act synergistically to diminish the effective tensile strength of the material. The interaction between normal and shear stresses promotes crack growth and facilitates the formation of additional micro-cracks, ultimately leading to premature failure of the material under applied loads. As a result, low tensile strength is observed in the presence of a notch (Fig. 16), which has been reported by Sharafisafa et al. (2008).

The findings reveal a significant influence of notches on the size effect in concrete specimens. As depicted in Fig. 16, the absence of notches exhibited a relatively lower size effect, indicating a more consistent mechanical response across different specimen sizes. In contrast, the presence of notches, particularly inclined notches, substantially increased the size effect. INT shows a significant size effect. Nevertheless, in smaller specimens, INT exhibits higher tensile strength when compared to the NC and INM. Conversely, INT experiences lower tensile strength in larger specimens compared to NC and INM. In larger specimens, the energy required to drive the crack forward is much greater, resulting in rapid crack propagation in the INT region (Fig. 17 (b)). On the other hand, in smaller specimens, despite early damage initiation in the INT region, the limited energy supply slows down the crack propagation process, resulting in delayed failure (Fig. 17 (a)). Apart from the presence of notches, the configuration of the notches also significantly influences the investigation of the size effect.

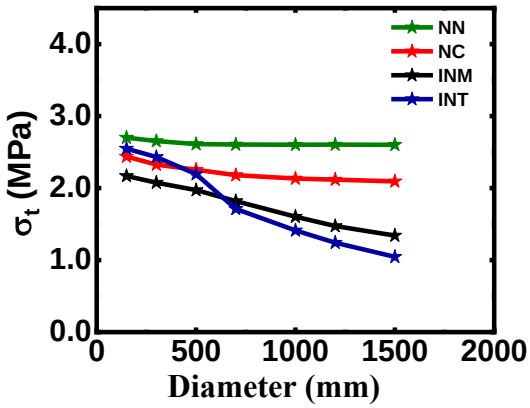

Fig. 16 The effect of a notch on tensile strength between specimens of different sizes.

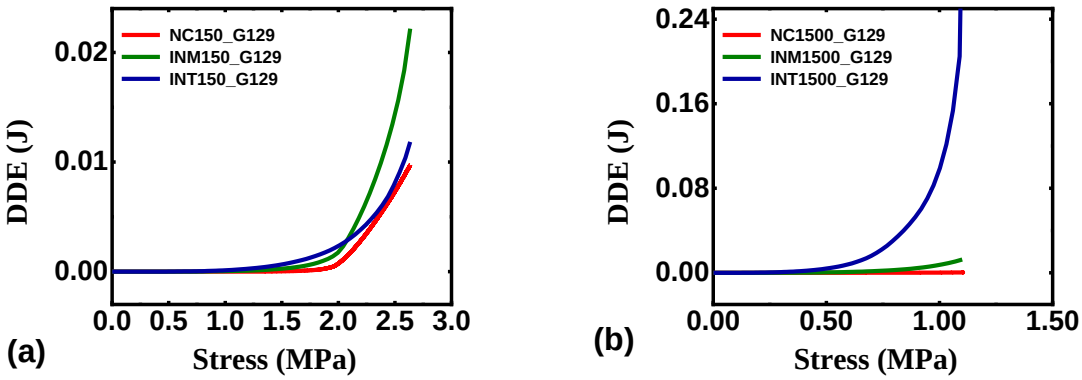

Fig. 17 The damage dissipation energy under split tension for (a) small and (b) large specimens.

5. Effect of Fracture energy in the size effect

The fracture energy plays a crucial role in influencing the tensile strength of concrete specimens. According to CEB-FIP (1991), $G_f = (0.0469d_a^2 - 0.5d_a + 26)\left(\frac{f}{10}\right)^{0.7}$ N/mm, where, d_a represents the maximum aggregate size. Higher fracture energy values were associated with greater tensile strengths, indicating improved crack resistance and enhanced tensile properties as shown in Fig. 18. Additionally, fracture energy significantly influences the size effect phenomenon in concrete. As the specimen size increases, the fracture energy required to drive crack propagation increases. This implies that larger specimens exhibit higher fracture energy values, which enhances their ability to withstand crack propagation and ultimately affects their size effect behavior. In

contrast, smaller specimens with lower fracture energy values demonstrate more pronounced size effect phenomena, with cracks propagating more rapidly due to the reduced energy required for crack initiation and growth.

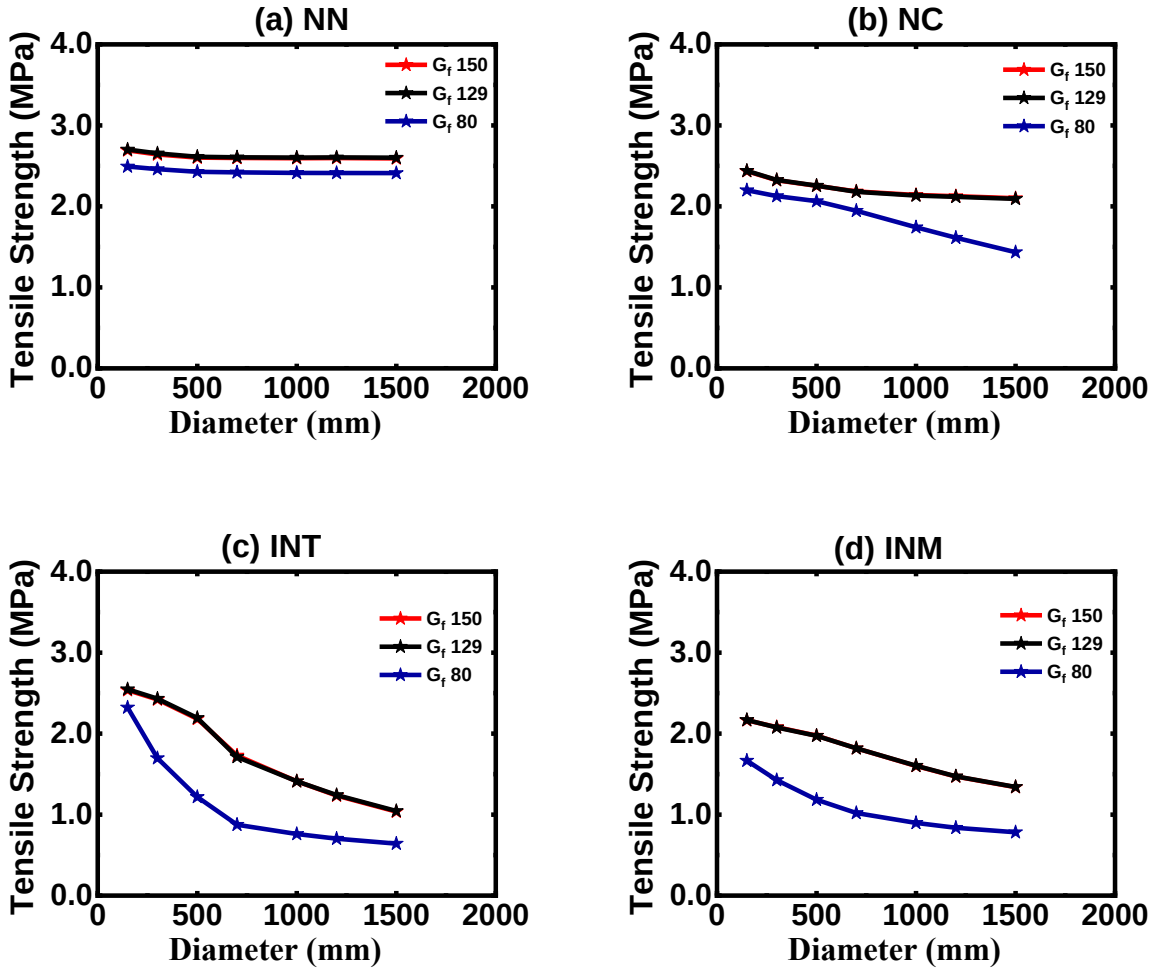

Fig. 18 The effect of fracture energy on tensile strength of different specimen sizes under different notch conditions.

5. CONCLUSIONS

This research comprehensively investigated the size effect phenomenon in the split tensile test of concrete. Experimental analysis was conducted on specimens with diameters of 150 mm, 300 mm, and 500 mm, considering maximum aggregate sizes of 10 mm. A minimal size effect was observed within this range.

Numerical simulations were performed on specimens with extended sizes ranging from 150 mm to 1500 mm in diameter to explore the size effect further. The numerical results closely agreed with the type 1 Size Effect Law (SEL) predictions. This alignment

between experimental and numerical analyses confirms the applicability of the size effect law to a broader range of specimen sizes. It strengthens the understanding of size-dependent behavior in materials.

Notches were added at different positions and angles to study the effect of crack geometry. It was observed that the presence of notches amplified the size effect, indicating that crack geometry plays a significant role in the overall mechanical response of the specimens. The orientation and placement of the notches were also found to affect the brittleness of the specimens, with inclined notches leading to higher brittleness.

Furthermore, the fracture energy of the specimens was varied to examine its effect on the size effect. Notably, it was discovered that specimens with lower fracture energy exhibited a more pronounced size effect. This suggests that as the fracture energy decreases, the larger specimens become more susceptible to brittle failure and exhibit a greater sensitivity to size effect.

These detailed investigations provide valuable insights into the complex interplay between specimen size, notch conditions, and crack geometry. These findings contribute to a better understanding of the mechanical response of concrete under different specimen sizes and provide valuable insights for designing and interpreting split tensile tests in practice.

REFERENCES

Abaqus Unified, F.E.A., (2009), software: Analysis user's manual, Volume III: Materials. Dassault Systèmes Simulia Corp., Providence, RI, USA.

Asadi, P., Fakhimi, A. and Ashrafi, M.J., (2023), "Dynamic tensile strength of rock specimens with different defect lengths", *Engineering Fracture Mechanics*, 284, p.109245.

Barr, B.I., Abusiaf, H.F. and Sener, S., (1998), "Size effect and fracture energy studies using compact compression specimens", *Materials and Structures*, **31**, pp.36-41.

Bažant, Z. P., and J. Planas. (1997), "Fracture and size effect in concrete and other quasibrittle materials." *London: CRC Press*

Bažant, Z. P., M. T. Kazemi, T. Hasegawa, and J. Mazars. (1991), "Size effect in Brazilian split-cylinder tests: Measurements and fracture analysis." *ACI Mater. J.* **88**(3): 325–332

Carmona, S., (2009), "Effect of specimen size and loading conditions on indirect tensile test results", *Materiales de Construcción*, **59**(294), pp.7-18.

CEB-FIP (Comité européen du béton-Fédération Internationale de la Précontrainte), "CEB-FIP model code 2010," fib Bulletin 55, Ernst & Sohn, Berlin.

Du, X., Jin, L. and Ma, G., (2013), "Meso-element equivalent method for the simulation of macro mechanical properties of concrete", *International Journal of Damage Mechanics*, **22**(5), pp.617-642.

Gregoire, D., Rojas-Solano, L.B. and Pijaudier-Cabot, G., (2012), "Continuum to discontinuum transition during failure in non-local damage models", *International Journal for Multiscale Computational Engineering*, **10**(6).

Grégoire, D., Rojas-Solano, L.B. and Pijaudier-Cabot, G., (2013), "Failure and size effect for notched and unnotched concrete beams", *International Journal for Numerical and Analytical Methods in Geomechanics*, **37**(10), pp.1434-1452

Häfner, S., Eckardt, S., Luther, T. and Könke, C., (2006), "Mesoscale modeling of concrete: Geometry and numerics", *Computers & structures*, **84**(7), pp.450-461.

Hasegawa, T., Shioya, T. and Okada, T., (1985), "Size effect on splitting tensile strength of concrete", *In Proceedings Japan Concrete Institute 7th Conference* (pp. 309-312).

Hoover, C.G. and Bažant, Z.P., (2014), "Universal size-shape effect law based on comprehensive concrete fracture tests", *Journal of engineering mechanics*, **140**(3), pp.473-479.

Ince, R. and Arici, E., (2004), "Size effect in bearing strength of concrete cubes", *Construction and Building Materials*, **18**(8), pp.603-609.

Jin, L., Yu, W. and Du, X., (2020), "Size effect on static splitting tensile strength of concrete: Experimental and numerical studies", *Journal of Materials in Civil Engineering*, **32**(10), p.04020308.

Jirásek, M., Rolshoven, S. and Grassl, P., (2004), "Size effect on fracture energy induced by non-locality", *International Journal for Numerical and Analytical Methods in Geomechanics*, **28**(7-8), pp.653-670.

Khaloo, A. R., M. R. Mohamadi Shooreh, and S. M. Askari. (2009), "Size influence of specimens and maximum aggregate on dam concrete: Compressive strength", *J. Mater. Civ. Eng.* **21** (8): 349–355

Kim, J.K., Yi, S.T. and Yang, E.I., (2000), "Size effect on flexural compressive strength of concrete specimens", *Structural Journal*, **97**(2), pp.291-296.

Krayani, A., Pijaudier-Cabot, G. and Dufour, F., (2009), "Boundary effect on weight function in non-local damage model", *Engineering Fracture Mechanics*, **76**(14), pp.2217-2231.

Lessard, M., Challal, O. and Aticin, P.C., (1993), "Testing high-strength concrete compressive strength", *Materials Journal*, **90**(4), pp.303-307.

Malhotra, V.M., (1976), "Are 4 x 8 inch concrete cylinders as good as 6 x 12 inch cylinders for quality control of concrete?", *In Journal Proceedings* (Vol. 73, No. 1, pp. 33-36).

Rocco, C., Guinea, G.V., Planas, J. and Elices, M., (1999), "Size effect and boundary conditions in the Brazilian test: Experimental verification", *Materials and Structures*, **32**, pp.210-217.

Sim, J.I., Yang, K.H. and Jeon, J.K., (2013), "Influence of aggregate size on the compressive size effect according to different concrete types", *Construction and building materials*, **44**, pp.716-725.

Simone, A., Askes, H. and Sluys, L.J., (2004), "Incorrect initiation and propagation of failure in non-local and gradient-enhanced media", *International journal of solids and structures*, **41**(2), pp.351-363.

Van Mier, J.G., (1996), Fracture processes of concrete (Vol. 12). CRC press.

Wang, L., L. Xing, and Y. Song. (2014), "Mesoscale modelling on size effect of splitting tensile strength and flexural compressive strength of concrete", *Eng. Mech.* **51** (10): 69–76

Wong, R.H. and Chau, K.T., (1998), "Crack coalescence in a rock-like material containing two cracks", *International Journal of Rock Mechanics and Mining Sciences*, **35**(2), pp.147-164

Zhang, N., (2016), “Size effect and failure characteristics on splitting tensile strength of concrete”, *DA Lian: Da Lian University of Technology*.

Zhou, F.P., Balendran, R.V. and Jeary, A.P., (1998), “Size effect on flexural, splitting tensile, and torsional strengths of high-strength concrete”, *Cement and Concrete Research*, **28**(12), pp.1725-1736.